

Study on the influence of rigid wall surface on the bubble characteristics of underwater explosion

L Meng¹, R Y Huang^{1*}, J Qin^{1,2}, J X Wang¹ and L T Liu¹

¹National Key Laboratory of Transient Physics, Nanjing University of Science and Technology, Nanjing 210094, China;

²Naval Research Academy, Beijing 100161, China

E-mail: ryhuang@njust.edu.cn

Abstract. In order to investigate the influence of rigid wall surface on the bubble characteristics of underwater explosion, the underwater explosion experiment under the boundary conditions of free surface and rigid wall surface was carried out on 2.5g cylindrical charge TNT in a 2×2×2m tank. The time history curves of shock wave and bubble pulsation were obtained by underwater pressure sensor, and the bubble pulsation process was observed by high-speed photography. The experimental results show that compared with the free surface underwater explosion, the shock wave peak pressure and the bubble pulse peak pressure in rigid wall surface underwater explosion are increased, and a large cavitation area appeared at the junction of rigid wall and water surface. After the bubbles contacted the rigid wall surface, the bubble morphology changed significantly, the first bubble pulsation period and the maximum radius of bubble expansion became larger. After the first bubble pulsation, the bubble partially collapsed and split into two parts, bubbles continued to pulsate in the direction of the rigid wall and the bottom of the water. Finally, combined with the experimental data of rigid wall surface at different explosion depths, the relationship between the first bubble pulsation period, the maximum bubble expansion radius and the explosion depth of 2.5gTNT under rigid wall conditions is given.

1. Introduction

In recent years, with the increasing application of underwater explosions in the field of defense industry, the research on the characteristics of bubble motion has gradually deepened, and the scope of research has also extended from simple free field single bubble pulsations to bubble group pulsations under complex boundary conditions[1-3]. After the actual explosive explodes, the formation, expansion, contraction, collapse, and jet of the bubble are always accompanied by interaction with the surrounding medium and structure, so it is an extremely complicated process[4-6], Only by fully revealing the influence of different factors on its motion characteristics and grasping its movement laws, can it better perfect the bubble mechanism and apply it reasonably to the national defense cause.

The bubble motion is particularly affected by the boundary conditions in underwater explosion, and the bubble motion exhibits different characteristics under free field, free surface, rigid wall surface,



and elastic boundary conditions [7-9]. Aiming at the motion and load characteristics of underwater explosion bubbles under different boundary conditions, scholars at home and abroad have carried out certain research work, which are mainly divided into experimental research and numerical simulation. In terms of experiments, Zhang Aman et al. [10] used electric sparks to generate bubbles, and used high-speed photography systems to experimentally observe and study the interaction between bubbles and the free liquid surface, and summarized the effects of free surface on the maximum bubble radius, pulsation period, jet time and jet width. Jin Hui et al. [11] carried out underwater explosion experiments under three conditions: free surface, near water bottom, and sink bottom explosion, and compared the bubble pulsation and secondary pulsation pressure. The experimental results show that the bottom boundary conditions have a greater impact on the secondary pulsation period of the near-bottom and sink bottom explosions. The pulsation period of the sink bottom explosion is greater than the near-bottom explosion, and the near-bottom explosion pulsation period is greater than the free surface explosion. In numerical simulation, Dong Qi et al. [12] used LS-DYNA to numerically simulate shallow water explosions at different explosion depths, and found that as the explosion depth increases, the bubble pulsation is less affected by the free surface and gravity, and more affected by the hydrostatic pressure and boundary surface. The direction of the jet produced by the contraction of the bubble is gradually changed from downward to upward, the arrival time of the maximum radius of the bubble and pulsation period also increase. Fang Bin et al. [13] used the finite element program MSC.Dytran to numerically simulate the pulsation process of underwater explosion bubbles under different boundary conditions. It was found that the boundary has a greater impact on the shape of the bubble, and the rigid wall surface will increase the pressure of bubble pulsation, but the free surface boundary has a small effect on the bubble pulsation pressure. Mu Jinlei et al. [14] also used the MSC.Dytran finite element software to simulate the dynamic characteristics of underwater explosion bubbles under different boundary conditions such as free surface in deep water, near free surface, near rigid wall surface and elastic boundary. When the distance from the boundary is approximately equal to the maximum radius of the bubble, the free surface will slightly reduce the maximum radius of the bubble, shorten the period, the effect of the rigid wall surface is opposite to free surface, and the effect of the elastic boundary is between the rigid wall surface and the free surface.

At present, experimental studies about the effects of boundary conditions on underwater explosions are mainly focused on conditions such as free field and near free surface, while the influence of rigid wall surface on the characteristics of bubbles in underwater explosion is mainly calculated by numerical simulation, and relative underwater explosion experiments under rigid walls are relatively few. In this paper, 2.5g TNT explosives are used to carry out underwater explosion experiments under free surface and under rigid plate to obtain various characteristic parameters of explosives under different working conditions. By comparing the pulsation process and load characteristics of bubbles under two boundary conditions, the effects of near free surface and rigid plate on the pulsation characteristics of underwater explosion bubbles are analyzed. On this basis, the distance between the explosive and the rigid plate was changed, and the influence of the explosion depth on the pulsation characteristics of the bubbles under the rigid plate was explored.

2. Underwater explosion experiment

The underwater explosion experiment was carried out in a $2\text{m} \times 2\text{m} \times 2\text{m}$ water tank of Jiangsu

Yongfeng Machinery Co., Ltd. The explosive was detonated with an industrial No. 8 electric detonator. The booster column was RDX-8701, and the main charge was TNT, specific dimensions and parameters are shown in table 1. The detonating device is tangled with 3M insulating tape, which can realize waterproofing for a short period of time while fixing the charge column. The explosive and detonating device are shown in figure 1.

Table 1. Size of explosives.

Explosive	W (g)	ρ ($\text{g}\cdot\text{cm}^{-3}$)	D (mm)	h (mm)
TNT	2.5	1.654	15	11.5
RDX-8701	0.3	1.667	5	9.2

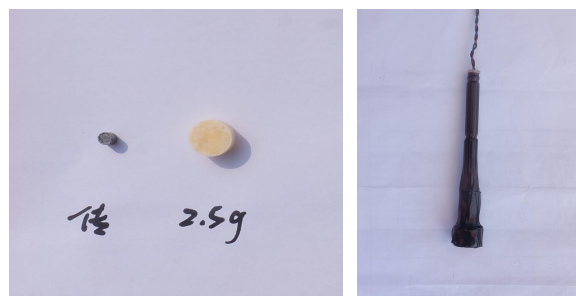


Figure 1. Explosives and detonating device.

First, the underwater explosion experiment of 2.5g TNT explosive was carried out at 1.0m depths below the free surface. The explosive is suspended in the center of the water tank, the distance from the bottom of the water tank is 0.8m, and the distance between the explosive and the free surface is $h=1.00\text{m}$. The size of h can be controlled by adjusting the height of the water level in the tank. Five PCB company-made 138A06 underwater explosion pressure sensors were placed at a distance of 0.3m, 0.4m, 0.5m, 0.6m, and 0.7m from the explosive, with a range of 34.475Mpa. A weighing scale with a weight of 1.5kg is hung directly below each sensor. The high-speed camera is 1.3m away from the explosion source, and an LED light source is installed on the top of the water tank for auxiliary lighting. The experimental device schematic diagram and field layout are shown in figure 2 and figure 3.

Secondly, the underwater explosion experiment of 2.5g TNT explosive was carried out at 0.28m depths below the free surface and rigid wall. Underwater explosion experiments on rigid wall surface were also performed in a $2\text{m}\times 2\text{m}\times 2\text{m}$ water tank. Explosives and explosive devices were consistent with free surface underwater explosion experiments. A $80\text{cm}\times 80\text{cm}\times 1\text{cm}$ rigid wall was placed in the center of the water tank, four support frames with a length of 1.0m were welded at the four corners of the steel wall, and a square steel plate with a side length of 30cm and a thickness of 1cm was welded at the bottom of each bracket as a counterweight so that the steel plate is fixed at the central area of the water surface. Adjust the surface height of the water in the water tank so that the lower surface of the steel plate just falls into the water. A thin wire is used to cross-fix the explosive directly below the center point of the steel plate, and the distance from the water surface is h . Two underwater explosion pressure sensors were placed in a straight line at a distance of 0.4m and 0.5m from the explosive, with a range of 34.475Mpa. Similarly, a 1.5kg weighing scale is hung directly under each sensor, and the

high-speed camera is 1.3m away from the explosion source. The experimental device schematic diagram and field layout are shown in figure 4 and figure 5.

Finally, in order to explore the effect of the explosion depth on the pulsation characteristics of the bubble, the rigid wall plate underwater explosion experiment were carried out with 2.5g TNT explosives at different depths. Changing the depth of the explosive by adjusting the position of the thin wire, the rigid wall plate underwater explosion experiment was performed at depths of 0.20m, 0.17m, 0.15m and 0.13m. An underwater explosion pressure sensor was placed 0.7m away from the explosive. The specific experimental arrangement is shown in table 2.

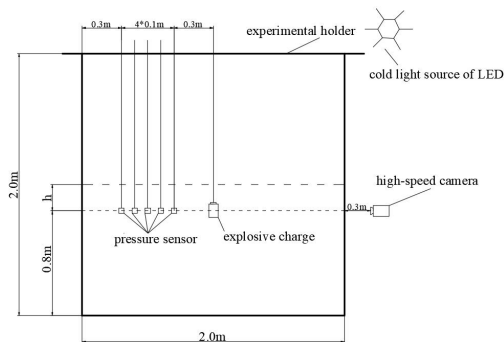


Figure 2. Schematic diagram of free surface experiment. **Figure 3.** Layout of free surface experiment.

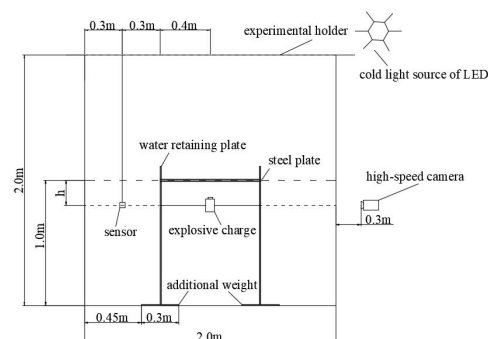


Figure 4. Schematic diagram of rigid plate experiment. **Figure 5.** Layout of rigid plate experiment.

Table 2. Experimental arrangement.

Number	Condition	h (m)	Sensor location (m)
1	Free surface	1.00	0.3/0.4/0.5/0.6/0.7
2	Free surface	0.28	0.4/0.5
3	Rigid plate	0.28	0.4/0.5
4	Rigid plate	0.20	0.7
5	Rigid plate	0.17	0.7
6	Rigid plate	0.15	0.7
7	Rigid plate	0.13	0.7

3. Experimental results and analysis

3.1. Experimental results

Taking the explosion at 1.0m below the free surface of 2.5g TNT explosive as an example, figure 6 shows the pressure time history curve measured by an underwater pressure sensor at different distances from the source of the explosion. It can be seen from the figure that after the shock wave propagates to the sensor, the pressure quickly reaches the peak value and then rapidly decays; at 37.19ms, the first bubble pulsation ends, and the sensor has a small peak due to the bubble pulsation; at 71.14ms, the second bubble pulsation ends, and the peak pressure of the bubble pulsation is reduced compared with the first bubble pulsation.

Figure 7 is the pressure time history curve of the shock wave at different distances from the explosion source. As can be seen from the figure, When the shock wave reaches the sensor at 0.3m, the timing starts, after 0.07ms, the shock wave reaches the sensor at 0.4m, so the propagation speed of the shock wave in the water is about 1430m/s. Comparing the peak pressure of shock waves at various measuring points under different burst distances, it is found that the peak pressure of the shock waves decays exponentially as the burst distance increases.

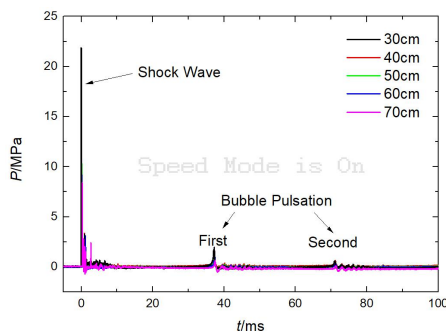


Figure 6. Pressure time history curve

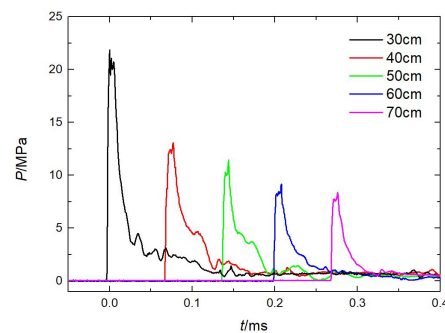


Figure 7. Pressure time history curve of shock wave.

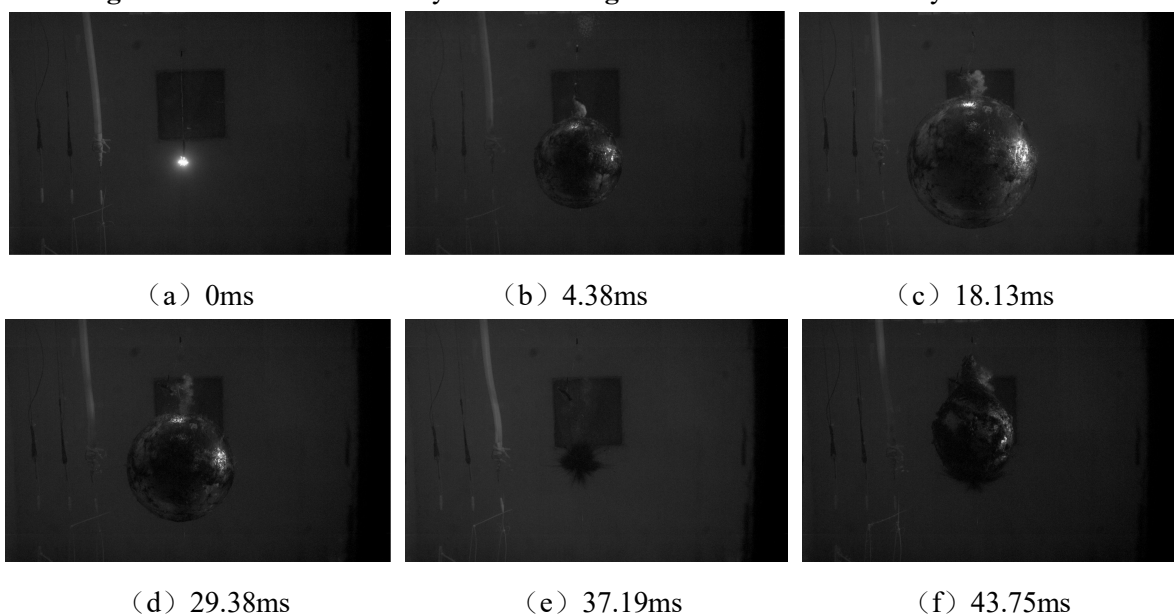


Figure 8. Bubble pulsation under free surface ($h=1.0m$).

Figure 8 shows the process of bubble generation, expansion and contraction in experiment No. 1. At $t=0\text{ms}$, the explosive explodes, releasing high-temperature and high-pressure gas, and the bubble expands rapidly; at $t=4.38\text{ms}$, the radius of the bubble has increased to 15cm , after which the bubble continues to expand, the pressure inside the bubble gradually decreases, and the expansion rate gradually decreases too. When the pressure in the bubble is equal to the pressure of the surrounding fluid, the bubble continues to expand due to the inertia of water; when $t=18.13\text{ms}$, the radius of the bubble reaches the maximum value ($R_{\text{max}}=22.30\text{cm}$), and the pressure in the bubble reaches the minimum value and is smaller than the water pressure outside the bubble. the bubble begin to shrink gradually; at $t=37.19\text{ms}$, the bubble radius is the smallest, and the second bubble pulsation starts. During the second pulsation of the bubble ($t=43.75\text{ms}$), it can be seen that part of the gas in the bubble is taken out from the bubble due to the action of the water jet. At the same time, the explosion products escape from the surface of the bubble during the pulse pulsation.

The damage of underwater weapon charges to targets mainly depends on the coupling of shock waves and bubble pulsations. Under the action of shock waves, the target usually undergoes local deformation or breakage, its damage effect mainly depends on the magnitude of its peak stress, and the damage of bubble pulsation mainly depends on the whip-like undulation of the target to cause overall damage, so the bubble pulse period, the maximum radius of bubble expansion and the size of bubble energy are particularly critical. Table 3 shows the experimental results of the shock wave peak pressure P_{m1} , the bubble pulsation peak pressure P_{m2} , the bubble pulsation period T , the bubble expansion maximum radius R_{max} , and the specific bubble energy E_b of the free surface and rigid wall underwater explosion experiments. Among them, the specific bubble energy E_b is calculated according to formula (1) [15].

$$E_b = \frac{0.6842 P_h^2 \rho_w^{\frac{3}{2}} T^3}{W \times 10^6} \quad (1)$$

In the formula:

E_b —Specific bubble energy, MJ/kg;

P_h —The sum of the hydrostatic pressure at the explosive center and the local atmospheric pressure, Pa;

ρ_w —Density of water, usually taken 1000 kg/m^3 for fresh water at room temperature;

T —Bubble pulsation period, s;

W —Explosive equivalent, kg.

Table 3. Experimental result.

Number	Condition	h (m)	R (m)	P_{m1} (MPa)	P_{m2} (MPa)	T (ms)	R_{max} (cm)	E_b (MJ/kg)
1	Free surface	1.00	0.3	21.85	2.03	37.19	22.30	1.79
			0.4	13.07	1.64			
			0.5	11.44	1.20			
			0.6	9.15	0.95			
			0.7	8.38	0.78			

2	Free surface	0.28	0.4	12.47	1.56	39.06	23.75	2.07
			0.5	10.45	1.05			
3	Rigid plate	0.28	0.4	12.95	1.75	40.63	26.65	2.33
			0.5	10.88	1.22			
4	Rigid plate	0.20	0.7	7.82	1.30	39.38	24.32	2.12
5	Rigid plate	0.17	0.7	7.70	1.27	39.19	24.20	2.09
6	Rigid plate	0.15	0.7	7.52	1.23	38.75	23.66	2.02
7	Rigid plate	0.13	0.7	7.15	1.17	38.13	23.29	1.93

3.2. Experimental validity verification

For the transmission of shock waves in free fields, Cole [16] summarized the empirical formula of underwater explosion shock waves through the collation of a large amount of experimental data in the early stage, and was widely recognized. Zamyshlyayev [17] improves on the basis of cole as:

$$P(t) = P_{m1} e^{-t/\theta} \quad (2)$$

$$P_{m1} = \begin{cases} 44.1 \times \left(\frac{\sqrt[3]{W}}{R} \right)^{1.5} & 6 \leq r \leq 12 \\ 52.4 \times \left(\frac{\sqrt[3]{W}}{R} \right)^{1.13} & 12 \leq r \leq 240 \end{cases} \quad (3)$$

$$\theta = \begin{cases} 0.45 R_0 r^{0.45} \times 10^{-3} & r \leq 30 \\ 3.5 \frac{R_0}{c_w} \sqrt{\lg r - 0.9} & r > 30 \end{cases} \quad (4)$$

$$I = 5768 \times \sqrt[3]{W} \left(\frac{\sqrt[3]{W}}{R} \right)^{0.89} \quad (5)$$

In the formula:

θ —The exponential decay time constant of the shock wave refers to the time required for the shock wave peak pressure P_{m1} to decay to P_{m1}/e , s;

R —Distance from measuring point to explosion, m;

R_0 —Explosive initial radius, m;

c_w —Sound speed in water, fresh water at room temperature is generally taken at 1460m/s;

r — R/R_0 ;

I —Specific impulse, N • s/m².

In the underwater explosion of TNT explosives, there are the following empirical formulas for the bubble pulsation period T and the maximum bubble expansion radius R_{max} [17]:

$$T = 2.11 \times \frac{W^{\frac{1}{3}}}{(h+10)^{\frac{5}{6}}} \quad (6)$$

$$R_{\max} = 3.5 \times \left(\frac{W}{h+10} \right)^{\frac{1}{3}} \quad (7)$$

In the formula: h is the water depth, m.

Table 4 shows the errors between the experimental values and empirical formula of P_{m1} , T , R_{\max} at 1.00m below the free surface. It can be seen from the table that the error of the shock wave peak pressure at each measurement point is small, and the average error is 6.15%; The error between the bubble pulsation period and the empirical formula is 4.20%, and the error between the maximum bubble expansion radius and the empirical formula is 4.40%. Since the appropriate range of the empirical formula is infinite waters, but the experiment in this paper is performed in a limited water area of $2\text{m} \times 2\text{m} \times 2\text{m}$, so the expansion of the bubble will be constrained by the surrounding walls, resulting in the experimental value being smaller than the theoretical value. On the whole, the shock wave and bubble pulsation characteristics are in good agreement with the empirical formula, and the errors are less than 10%, which verifies the authenticity and reliability of the experiment.

Table 4. Error between experiment and empirical formula.

Character	R (m)	Experimental (MPa)	Empirical (MPa)	Error (%)	Average error (%)
P_{m1}	0.3	21.85	21.38	2.20	6.15
	0.4	13.07	15.45	15.40	
	0.5	11.44	12.01	4.75	
	0.6	9.15	9.77	6.35	
	0.7	8.38	8.21	2.07	
T		37.19	38.82	4.20	
R_{\max}		22.30	21.36	4.40	

4. Effects of different boundary conditions on the pulsation characteristics of underwater explosion bubbles

When explosives explode near the free surface and near the wall surface, due to the presence of water or rigid walls, the flow field characteristics around the charge are changed, which makes the physical movement process of the bubbles and the law of load more complicated [19]. Because this is a complex explosion dynamics problem involving water and boundary effects, the theoretical research in this area is still relatively immature. In terms of experiments, people generally observe bubble pulsation under different boundary conditions through high-speed photography, so as to qualitatively analyze the influence of different boundary conditions on bubble pulsation.

4.1 Free surface

When the bubble moves near the boundary of the free surface, the existence of the water surface will make the bubble non-spherical, and then a Bjerknes-type concave jet is generated, and the pulsation period is also changed relative to the free field [10].

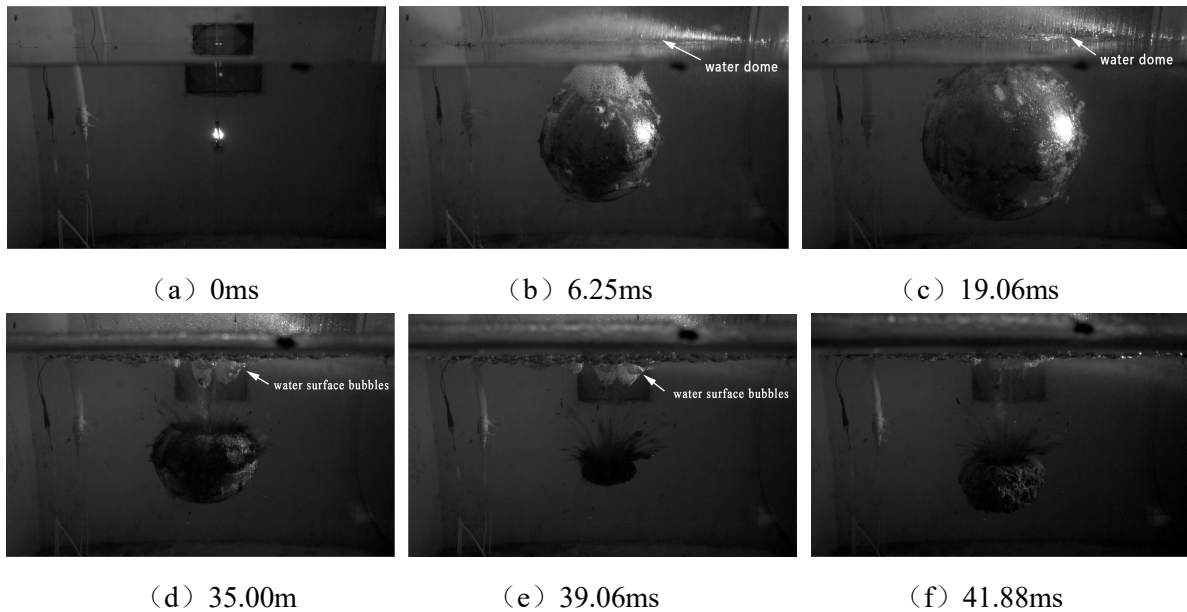


Figure 9. Bubble pulsation under free surface ($h=0.28\text{m}$).

Figure 9 shows the formation, expansion and contraction of bubbles at 0.28m below the free surface of 2.5g TNT explosive. After the charge exploded, the bubble rapidly expanded in a spherical shape. When the upper surface of the bubble approached the free liquid surface ($t=6.25\text{ms}$), the spherical bubble began to evolve into an oval bubble, water droplets splashing upward form a water dome above the water surface, and the height of the water dome decreases as the distance from the center of the bubble increases; After that, the bubble continued to expand and moved upward. When $t=19.06\text{ms}$, the bubble expanded to the maximum, its upper surface was close to the water surface and the whole bubble was oval, the upper and lower diameters were slightly larger than the left and right diameters, the corresponding water surface phenomenon was still in the form of a water dome; After that, the bubble began to shrink downward. During the shrinking process ($t=35.00\text{ms}$), the reflow speed of the top fluid was higher than the bottom, so a downward jet was formed. The upper boundary of the bubble starts to sag from the flat to the inside, and the trajectory of the release of detonation product gas can be observed around the recessed area. At the same time, the water jet drives part of the gas into the water surface to form water surface bubbles; When $t=39.06\text{ms}$, the first pulsation ends, the bubbles contract to a minimum, and the overall shape is flat, water surface bubbles still exist at this time; After that, the bubble continued to move downward and began to expand a second time, the bubble no longer became spherical, but had a flat upper boundary, and there was no longer a smooth interface between the bubble and water ($t=41.88\text{ms}$).

In the meantime, comparing the experimental data in table 3, it can be seen that when the charge depth is reduced from 1.0m to 0.28m, the distance between the explosive and the free surface decreases, the influence of the free surface boundary on the bubble pulsation increases, and the bubble pulsation period, the bubble expansion maximum radius increases. Comparing the peak pressure of the shock wave and the peak pressure of the bubble pulsation at 0.4m and 0.5m from the explosion source, it is found that the P_{m1} and P_{m1} both decreased with the charge depth.

4.2 Rigid plate

When bubbles pulsate near the structure surface, they are slightly repelled by the structure surface during the expansion phase, and are strongly attracted by the structure during the collapse phase [20]. Generally, due to the Bjerknes force, bubbles will be attracted by the structure in the water and move to the structure. Under the influence of buoyancy, inertia and other factors, high-speed jets will be formed along the direction of bubble collapse, and the jet will penetrate the bubble and impact the other side of the bubble wall, and eventually act on the structure and cause structural damage.

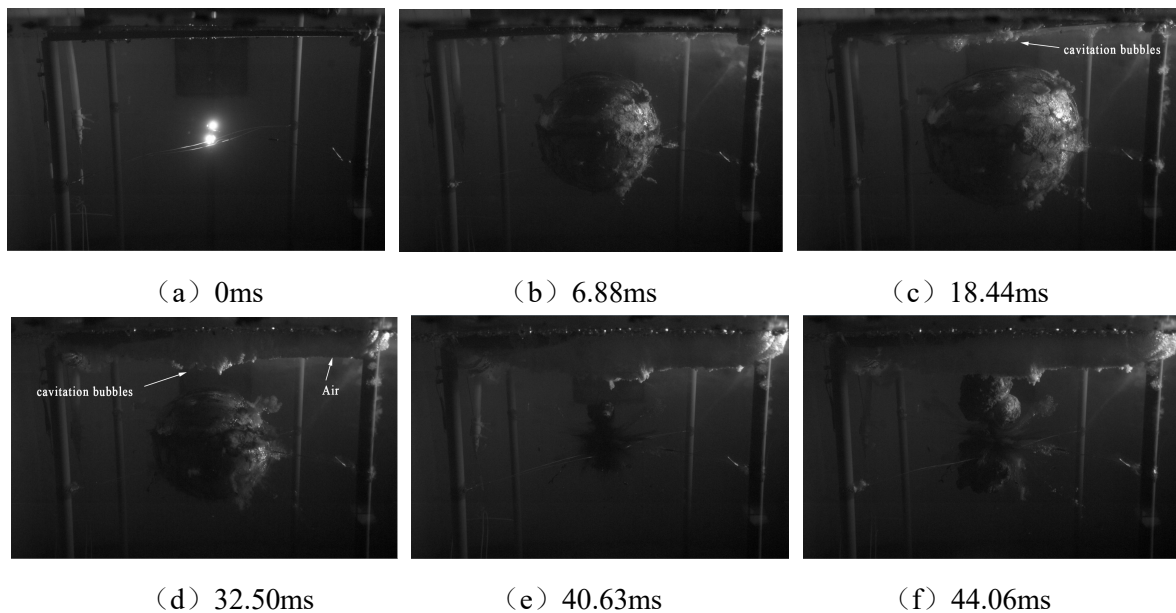


Figure 10. Bubble pulsation under rigid plate ($h=0.28\text{m}$).

Figure 9 shows the bubble generation, expansion, and contraction of 2.5g TNT explosive at 0.28m below the rigid wall. After the charge exploded, the bubbles rapidly expanded and moved upward in a spherical shape. During the expansion process, air pockets appeared at the junction between the rigid wall and the water surface (as shown in figure 10 (b). Air pockets consist of many small bubbles, also called cavitation bubble layer), and the air pockets gradually increases with time. When $t=18.44\text{ms}$, the bubble expands to the maximum, its upper surface is flat by the repulsion of the rigid wall, and the left and right diameters are larger than the upper and lower diameters, the upward movement of the bubble is suppressed at this time; After that, the bubble starts to shrink downward. During the shrinkage process, part of the air around the rigid wall surface is sucked under the steel plate due to the backflow of the fluid, and some of the gas on the bubble surface overflows (figure 10(d)); When $t=40.63\text{ms}$, the first pulsation ends, the bubble shrinks to a minimum, and a water jet is generated in the upward direction. The trajectory of the detonation product gas released outward can be observed below the bubble, the volume of air sucked under the rigid wall reaches the maximum at this time; After that, the second pulsation started, and the bubble partially collapsed and split into two parts, some of the bubbles expanded upward in an irregular spherical shape, and the other part was reversed, the interface between the two bubbles and water is no longer smooth (figure 10 (f)).

In addition, comparing the experimental data in table 3, it can be seen that when the explosion

depth remains constant and the boundary conditions change from a free surface to a rigid wall surface, the peak pressure of shock wave, peak pressure of bubble pulsation, bubble pulsation period and maximum radius of bubble expansion all increase.

5. Effects of rigid plate on pulsation characteristics of underwater explosion bubbles at different depths

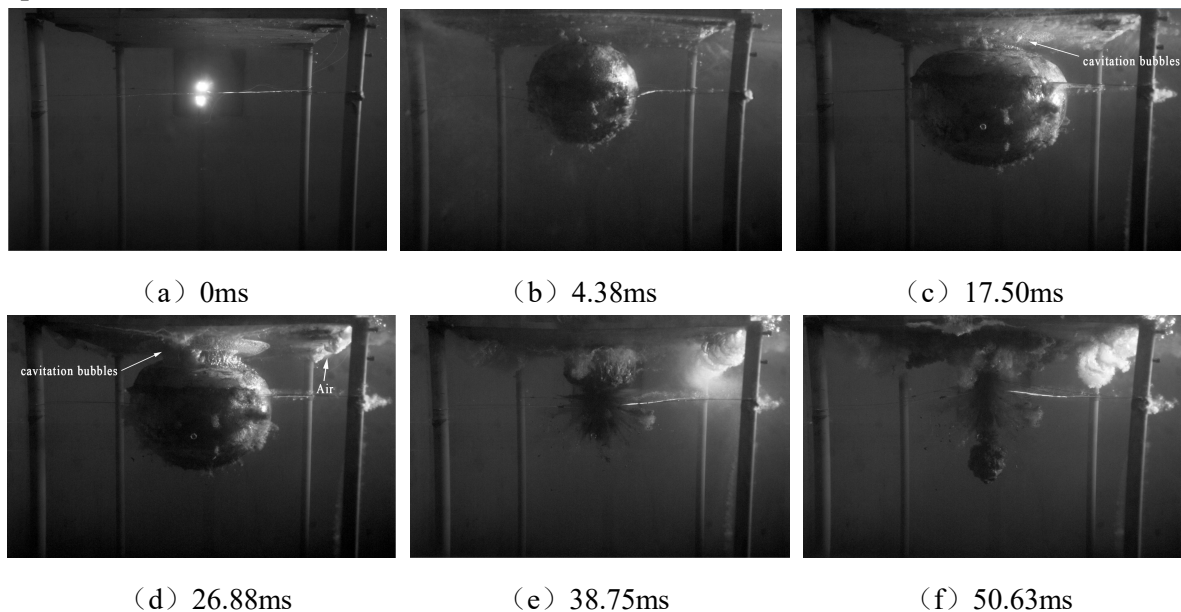


Figure 11. Bubble pulsation under rigid plate ($h=0.15\text{m}$).

Figure 11 shows the bubble generation, expansion and contraction of 2.5g TNT explosive at 0.15m below the rigid wall. After the charge explosion, the bubble rapidly expands in a spherical shape and moves upward, because the distance between the explosion point and the rigid wall is small, the expansion of the upper bubble is inhibited by the rigid wall, the upward movement is slowed (figure 11 (b)); During the expansion process, air pockets appear at the junction between the rigid wall and the water surface, and gradually increase with time. When $t=17.50\text{ms}$, the bubble expands to the maximum, and its upper surface is flattened by the repulsion of the rigid wall surface, the left and right diameters are larger than the upper and lower diameters, also the center of the bubble is lower than the starting position at this time; After that, the bubble begins to shrink, during the shrinking process, the bubble moves upward due to the adsorption of the rigid wall. At $t=26.88\text{ms}$, the bubble contact the air pockets, the pressure inside the bubble decreases sharply, causing the bubble to shrink faster, part of the gas on the surface of the bubble overflows, and the secondary expansion of the air pocket occurs at the interface between the air pocket and the rigid wall, part of the air is sucked under the steel plate at this moment; When $t=38.75\text{ms}$, the first pulsation ends, the gas volume of the bubbles and air pockets shrinks to a minimum, and an upward water jet is generated below the bubble, the trajectory of the detonation product gas released outward can be observed; After the bubble collapses, part of the gas and air pockets converge under the rigid wall and diffuse to the surroundings, while another part of the gas continues to expand downwards, the surface of the bubbles is no longer smooth (figure 11 (f)).

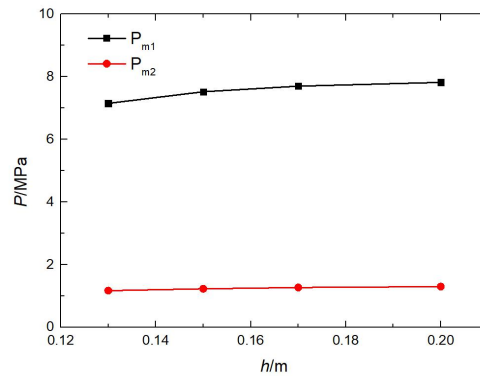


Figure 12. P_{m1} , P_{m2} at different explosion depths.

Figure 12 shows the shock wave peak pressure P_{m1} and bubble pulsation peak pressure P_{m2} of 2.5g TNT at different depths under a rigid wall. It can be seen from the figure that as the explosion depth increases, both the peak pressure of the shock wave and the peak pressure of the bubble pulsation increase, but on the whole, the impact of explosion depth on shock wave peak pressure is more significant, while the impact on bubble pulsation peak pressure is smaller.

Figure 13 shows the relationship between the first bubble pulsation period and the explosion depth in rigid wall underwater explosion experiment. Figure 14 shows the relationship between the maximum bubble expansion radius and the explosion depth. It can be seen from the figure that with the increase of the explosion depth, the first pulsation period and the maximum bubble expansion radius gradually increase, and both of them have a power function relationship with the explosion depth. Therefore, a power function is used to fit the experimental data, and the functional relationship between P_{m1} , P_{m2} and h is obtained. Among them, T_0 and R_{max0} are the first bubble pulsation and bubble expansion maximum radius calculated by the empirical formula when the explosion depth is 1.0m in the free field.

$$T = 1.21T_0 \times h^{0.08} \tag{8}$$

$$R_{max} = 1.76R_{max0} \times h^{0.17} \tag{9}$$

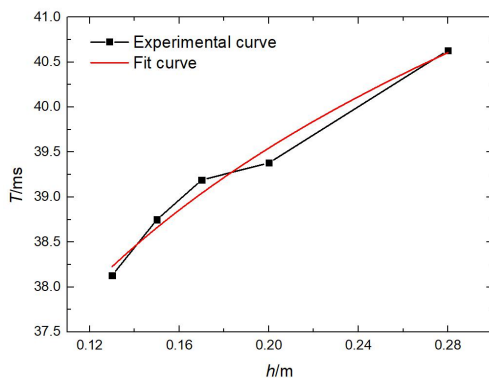


Figure 13. T - h curve.

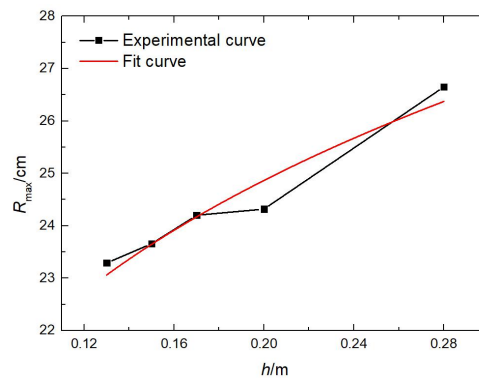


Figure 14. R_{max} - h curve.

6. Conclusion

By conducting underwater explosion experiments on 2.5g cylindrically charged TNT under two boundary conditions, the shock wave and bubble pulsation pressure time-history curves under different working conditions and the corresponding bubble pulsation process are obtained. Comparing the parameters under the two boundary conditions, the following conclusions are obtained:

(1) Compared with the free-field underwater explosion, the peak pressure of the shock wave and the peak pressure of bubble pulsation near the free surface are smaller, but the first bubble pulsation period and the maximum bubble expansion radius become larger. Due to the interaction of the bubble with the water surface, the bubble began to move downward during the contraction phase of the first pulsation and produced a Bjerknes-type concave jet.

(2) When the explosion depth remains constant and the boundary conditions change from a free surface to a rigid wall surface, the peak pressure of the shock wave, the peak pressure of the bubble pulsation, the bubble pulsation period, and the maximum radius of bubble expansion all increase. The existence of the rigid wall surface makes the bubbles slightly repelled during the expansion phase, and is strongly attracted by the structure during the collapse phase. After the first pulsation of the bubbles, the bubbles partially collapse and form a jet. After that, the bubble split into two and continued to pulse in two directions.

(3) Under rigid wall surface condition, the peak pressure of the shock wave, the peak pressure of the bubble pulsation, the bubble pulsation period and the maximum radius of bubble expansion all increase with the explosion depth. Based on the experimental data, the functional relationship between P_{m1} , P_{m2} and h of 2.5g TNT is obtained in this paper.

References

- (1) Hsu C Y, Liang C C and Nguyen A T 2014 *Ocean Engineering* **81** 29-38
- (2) Prior M K and Brown D J 2010 *IEEE Journal of Oceanic Engineering* **35**(1) 103-12
- (3) Wang L, Wang N and Zhang L 2012 *Propellants, Explosives, Pyrotechnics* **37**(1) 83-92
- (4) Wang Q S, Nie J X and Jiao Q J 2016 *Acta Armamentarii* **37**(S2) 23-8
- (5) Zhang A M, Wang S P and Huang C 2013 *European Journal of Mechanics - B/Fluids* **42** 69-91
- (6) Klaseboer E, Hung K C and Wang C 2005 *Journal of Fluid Mechanics* **537**(-1) 387
- (7) Zhang Z F, Wang C and Zhang A M 2019 SPH-BEM simulation of underwater explosion and bubble dynamics near rigid wall *Science China Technological Sciences*
- (8) Jia-Xia W, Zhi Z and Kun L 2018 *Applied Ocean Research* **78** 50-60
- (9) Lind S J 2010 Numerical study of the effect of viscoelasticity on cavitation and bubble dynamics *Dissertations & Theses - Gradworks*
- (10) Zhang A M, Wang C and Wang S P 2012 *Acta Physica Sinica* **61**(08) 300-12
- (11) Jin H, Zhang Q M and Gao C S 2009 *Acta Armamentarii* **30**(S2) 213-7
- (12) Dong Q, Wei Z B and Tang T 2018 *Chinese Journal of High Pressure Physics* **32**(02) 85-93
- (13) Mou J L, Zhu S J and Diao A M 2014 *Journal of Vibration and Shock* **33**(13) 92-7
- (14) Fang B and Zhu X 2008 *Journal of Naval University of Engineering* **20**(02) 85-90+112
- (15) Li J, Lin X K and Rong J L 2014 *Journal of Vibration and Shock* **33**(15) 200-5
- (16) Cole R H 1965 *Underwater explosions* New York: Dover Publications INC
- (17) Zamyshlyayev B V and Yakovlev Y S 1973 *Dynamic Loads in Underwater Explosion*

- (18) Zhou L and Xu G G 2003 *Chinese Journal of Explosives & Propellants* **26**(01):30-2 36
- (19) Shu-Shan W , Mei Land Feng M 2014 *Acta Physica Sinica* **63**(19) 182-90
- (20) Ni B Y, Li S and Zhang A M 2013 *Acta Physica Sinica* **62**(12) 345-55